Electronic Supplementary Material (ESI) for Journal of Materials Chemistry C.

Electronic Supplementary Material (ESI) for Journal of Materials Chemistry C.
This journal is © The Royal Society of Chemistry 2018

Supplementary Information

Laser-irradiated Inclined Metal Nanocolumns for Selective, Scalable, and Room-temperature Synthesis of Plasmonic Isotropic Nanospheres

Myoung-Sub Noh,[ab] Soo Deok Han,[abc] Songhwa Chae,[d] Seung Hyuk Back,[ab] Sangtae Kim,[b] Seung-Hyub Baek,[bf] Seong Keun Kim,[b] Ji-Won Choi,[b] Jin-Sang Kim,[b] Dong June Ahn,[ae] Dukhyun Choi,*[bd] and Chong-Yun Kang*[ab]

*Corresponding Author email address: dchoi@khu.ac.kr, cykang@kist.re.kr

1. FE-SEM images of Au thin films on sapphire at the various deposition angle.

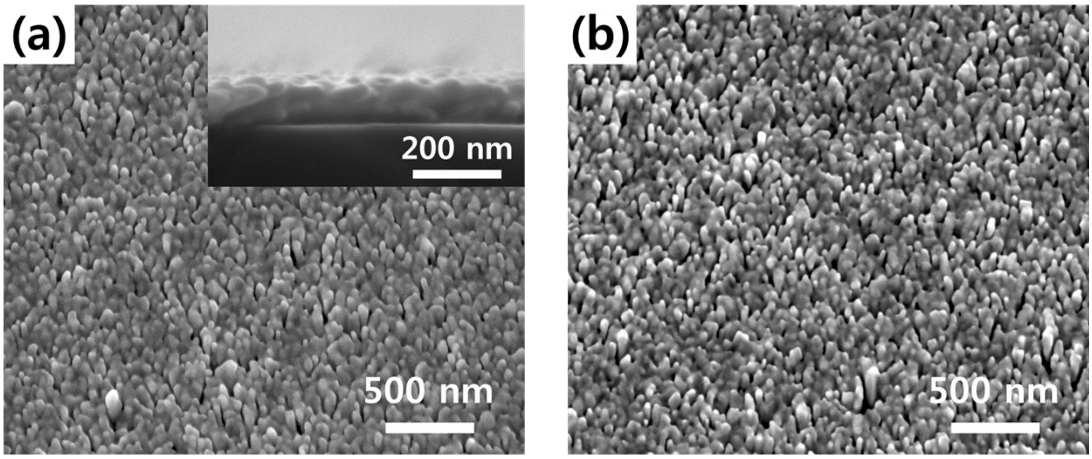

Fig. S1. The as-deposited Au nanostructures at the deposition angle of (a) 75° and (b) 80°. The inset shows the cross-sectional image of the deposited film.

2. XRD and EDX analysis of the AuNC on sapphire.

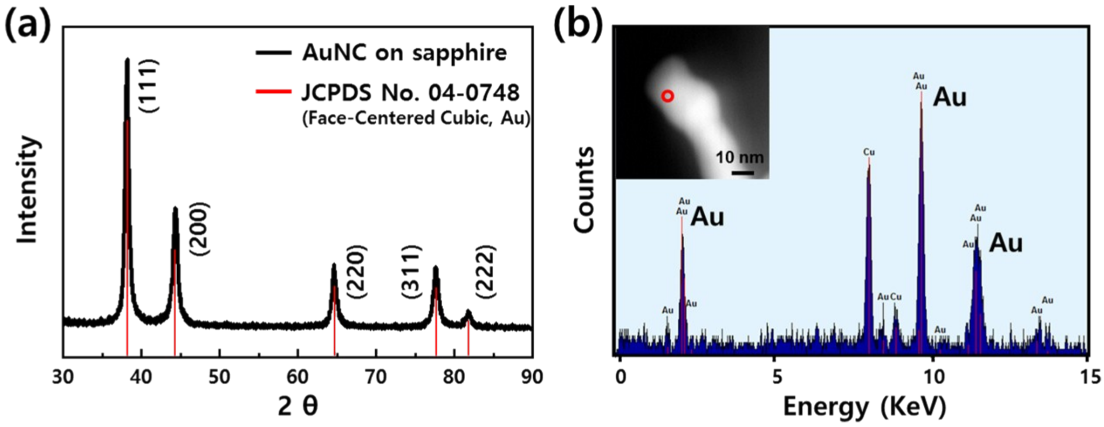

Fig. S2. (a) X-ray diffraction pattern of AuNC on sapphire and JCPDS No. 04-0748 (b) EDX spectrum of AuNC on sapphire.

3. HRTEM images of the AuNC and AuNS.

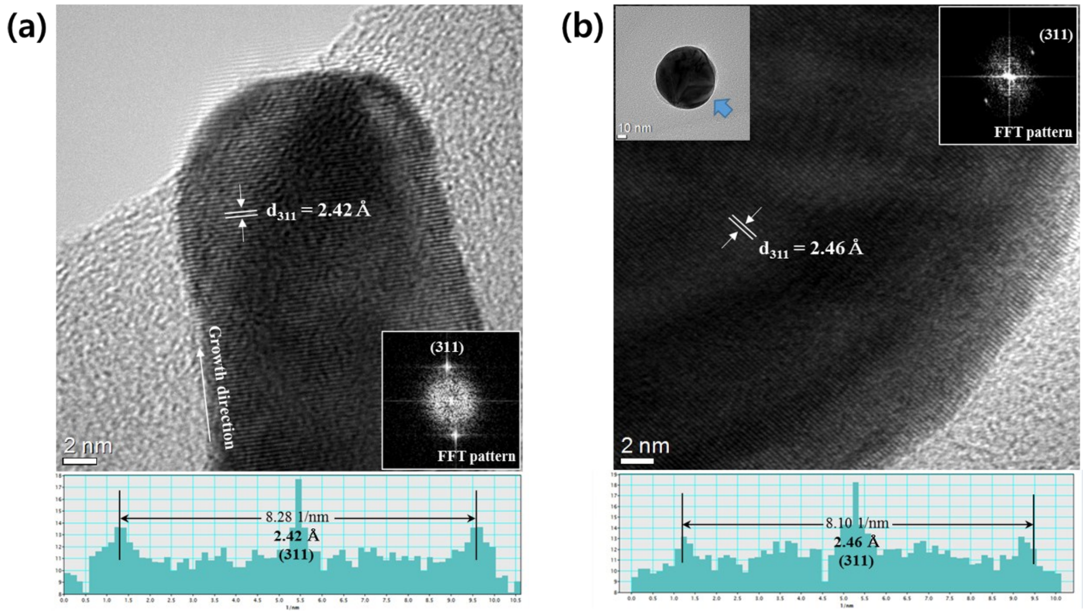

Fig. S3. HRTEM images of the lattice plane spacing in (a) AuNC and (b) AuNS. The measured lattices were 2.42 Å and 2.46 Å, which corresponds to the (311) planes. (Scale bars= 2 nm)

4. FE-SEM images of AuNC on sapphire after laser irradiation.

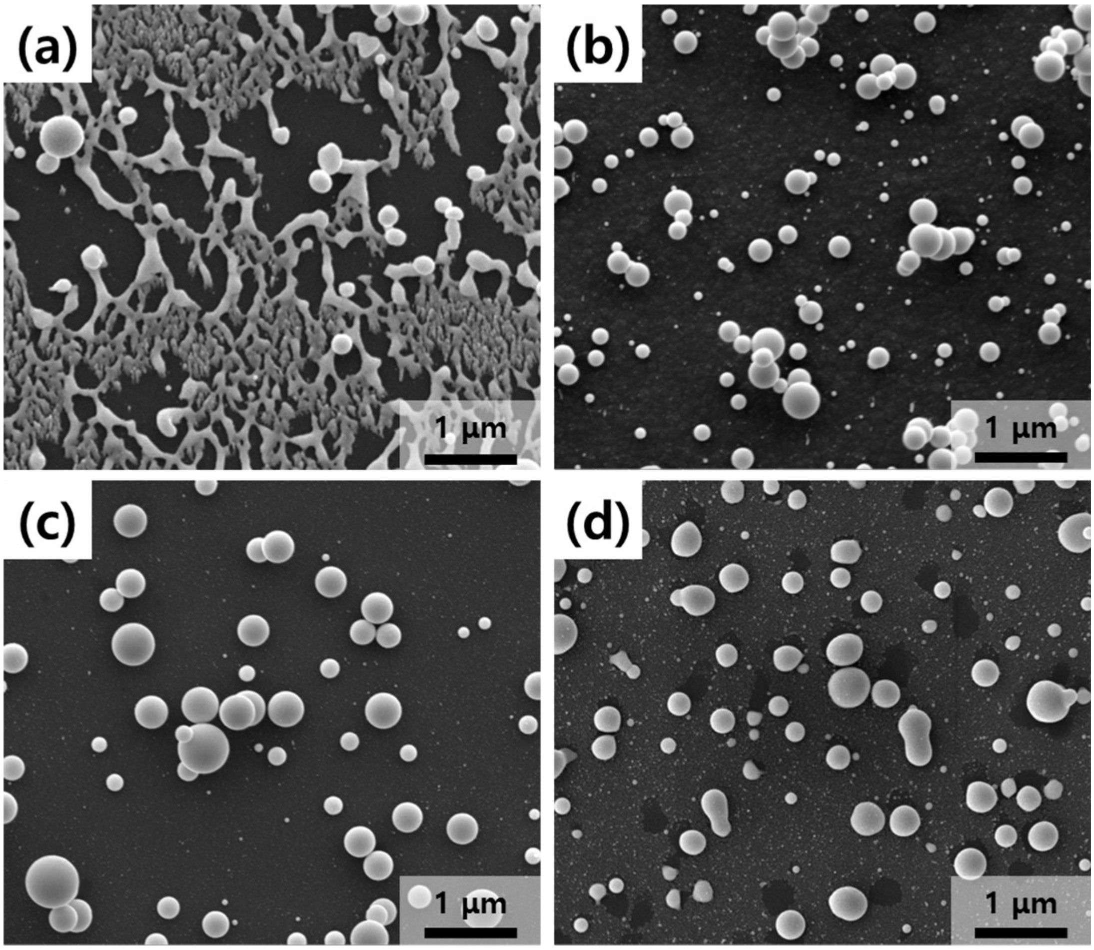

Fig. S4. Surface morphology of laser treated Au nanostructures on sapphire, as a function of the laser energy density of (a) 50 mJ·cm^{-2}, (b) 75 mJ·cm^{-2}, (c) 100 mJ·cm^{-2}, and (d) 150 mJ·cm^{-2}.

5. FE-SEM images of Au nanostructure after thermal annealing.

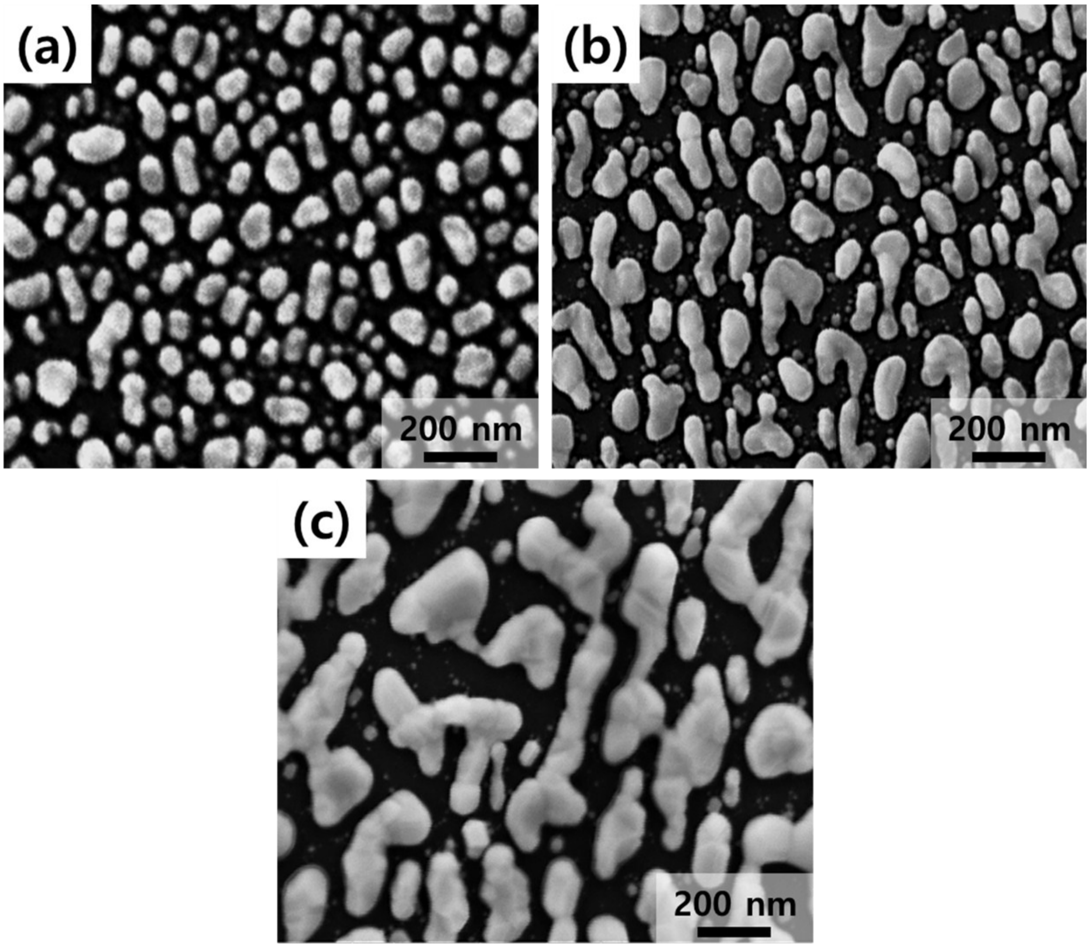

Fig. S5. Surface morphology of Au nanostructures thermally annealed for 1 h at (a) 100℃, (b) 200℃, (c) 300℃.

6. FE-SEM images of Au nanospheres after the laser irradiation

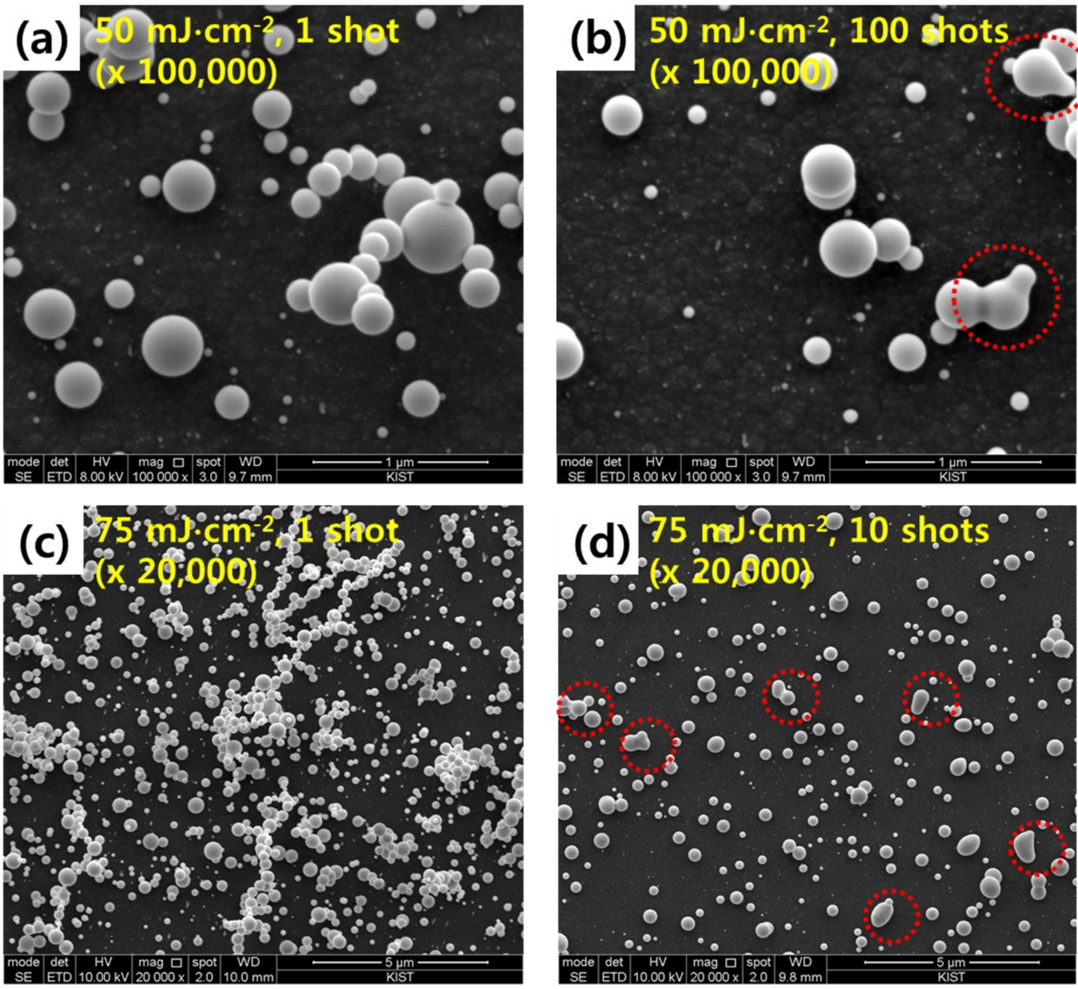

Fig. S6. Repeated laser irradiation induces coarsening and merging of individual AuNS (a) 50 mJ·cm^{-1}, 1 shots, (b) 50 mJ·cm^{-1}, 100 shots, (c) 75 mJ·cm^{-1}, 1 shots, (d) 75 mJ·cm^{-1}, 10 shots,

7. Change in the heat transfer and the maximum temperature as a function of laser irradiation time using COMSOL Multiphysics simulation.

Irradiation Time [ns]	0.1	1	10	
3D view		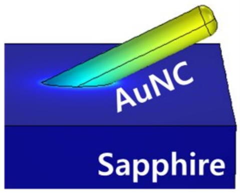	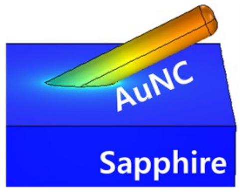	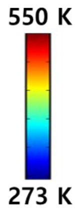
Max temp. [K]	362	452	486	
Irradiation Time [ns]	20	23.9	24	
3D view	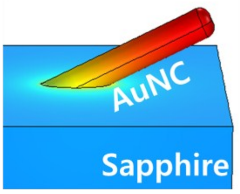	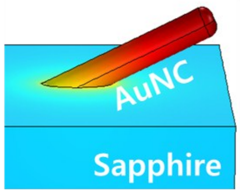	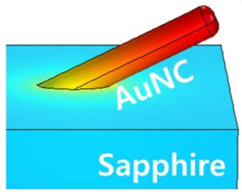	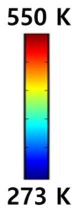
Max temp. [K]	521	535	520	

Fig. S7. Change in the heat transfer and the maximum temperature as a function of laser irradiation time on AuNC/Sapphire structures, defined using COMSOL Multiphysics.

8. Contact angle properties as a function of kinds of the substrates.

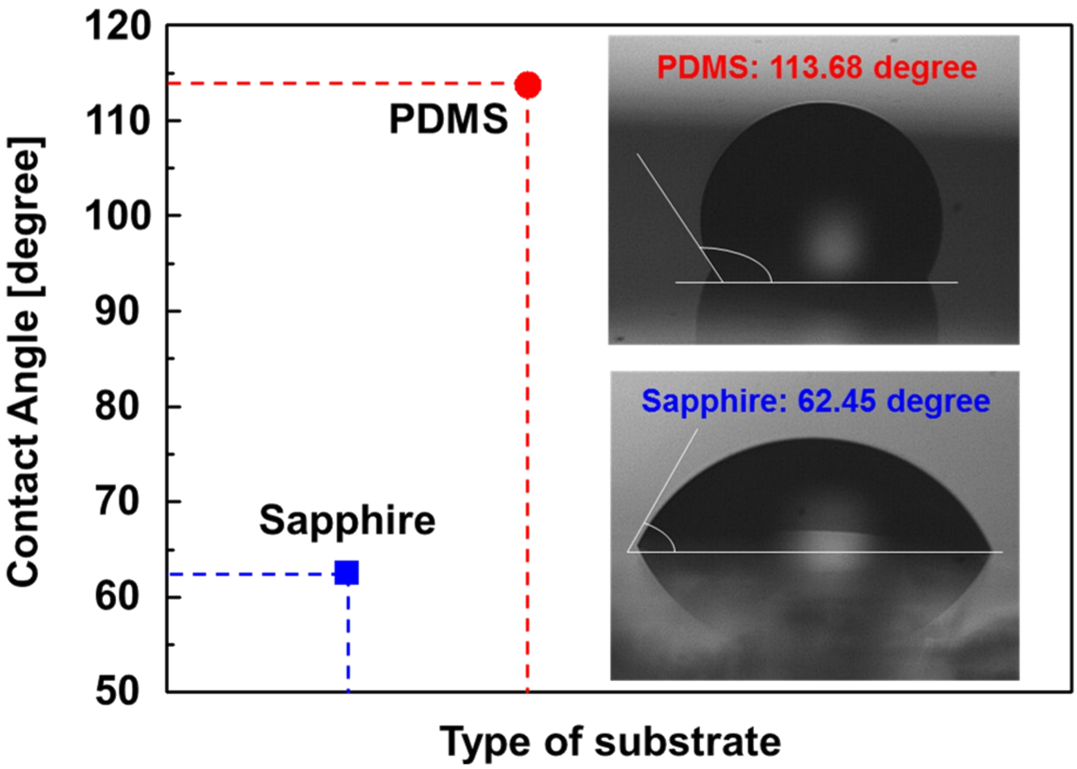

Fig. S8. Contact angle properties as a function of kinds of the substrates.

To explain that the diameter of the AuNCs affects the size of the finally fabricated AuNSs, we measured the contact angle of the substrates. It can be seen that sapphire substrate has greater surface energy than the PDMS substrate, since contact angle and surface energy are inversely proportional to each other. In addition, the adatom diffusion increases when the substrate has a high surface energy. For this reason, larger diameter AuNCs are fabricated on the sapphire substrate than on the PDMS substrate, and the AuNC deposition on the sapphire substrate is dense. Finally, after laser irradiation, the diameter of the AuNSs fabricated on the sapphire substrate fabricated is larger than that of the AuNSs on a PDMS substrate.

9. XRD and EDX analysis of the AuNC on PDMS.

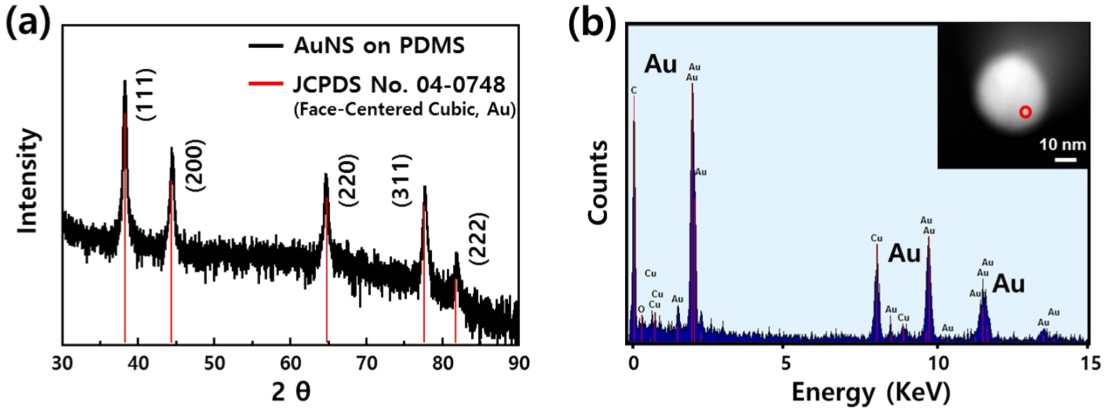

Fig. S9. (a) X-ray diffraction pattern of AuNC on PDMS and JCPDS No. 04-0748 (b) EDX spectrum of AuNC on PDMS.

10. HRTEM images of the AuNC and AuNS.

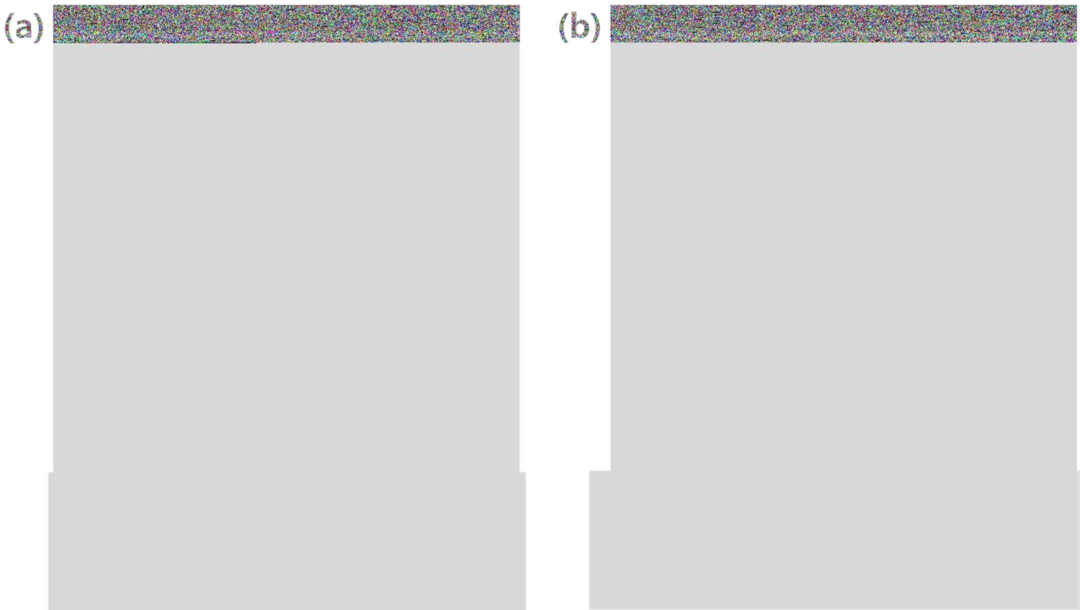

Fig. S10. HRTEM images of the lattice plane spacing in (a) AuNC and (b) AuNS. The measured lattices were 2.42 Å and 2.46 Å, which corresponds to the (311) planes. (Scale bars= 2 nm)

11. FE-SEM images of AuNC on PDMS after laser irradiation.

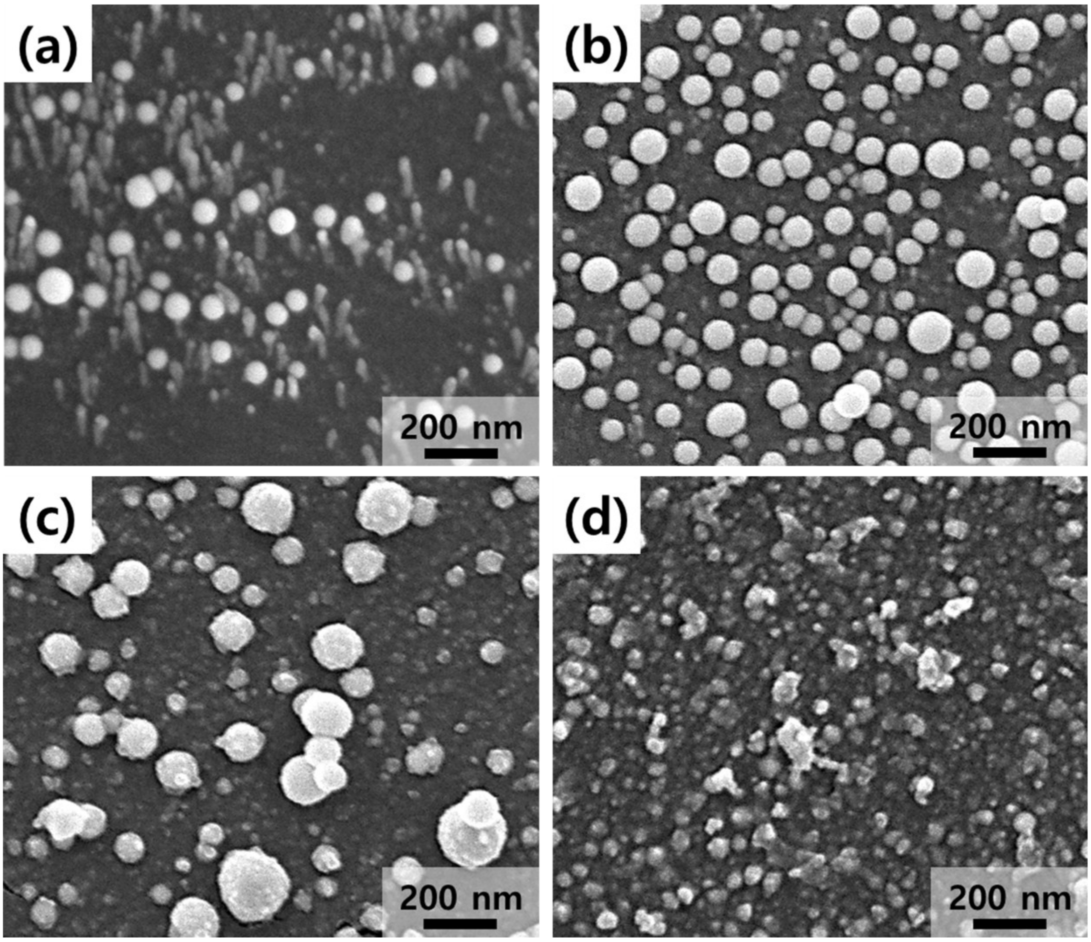

Fig. S11. Surface morphology of laser treated Au nanostructures on PDMS, as a function of the laser energy density of (a) 25 mJ·cm^{-2}, (b) 35 mJ·cm^{-2}, (c) 50 mJ·cm^{-2}, and (d) 100 mJ·cm^{-2}.

12. Optical properties of the photoresist mask.

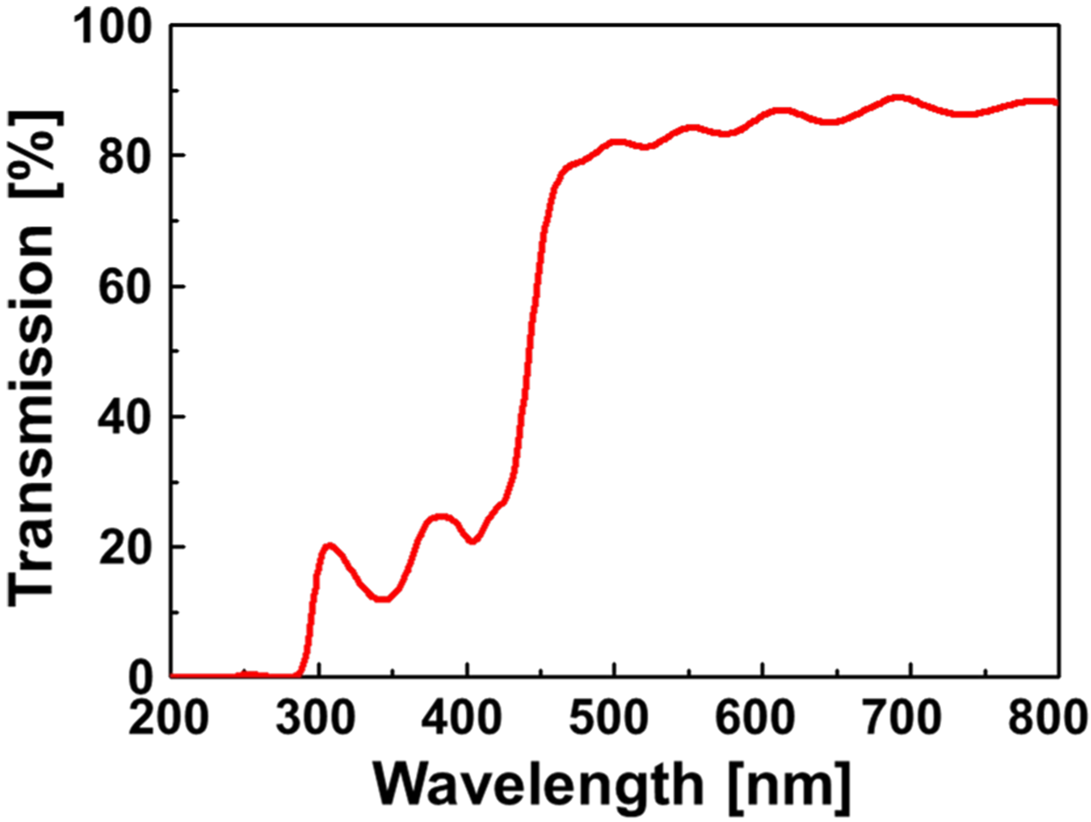

Fig. S12. Optical properties of the photoresist mask (Positive PR: GXR601)

13. Details of the "KIST" patterning processes.

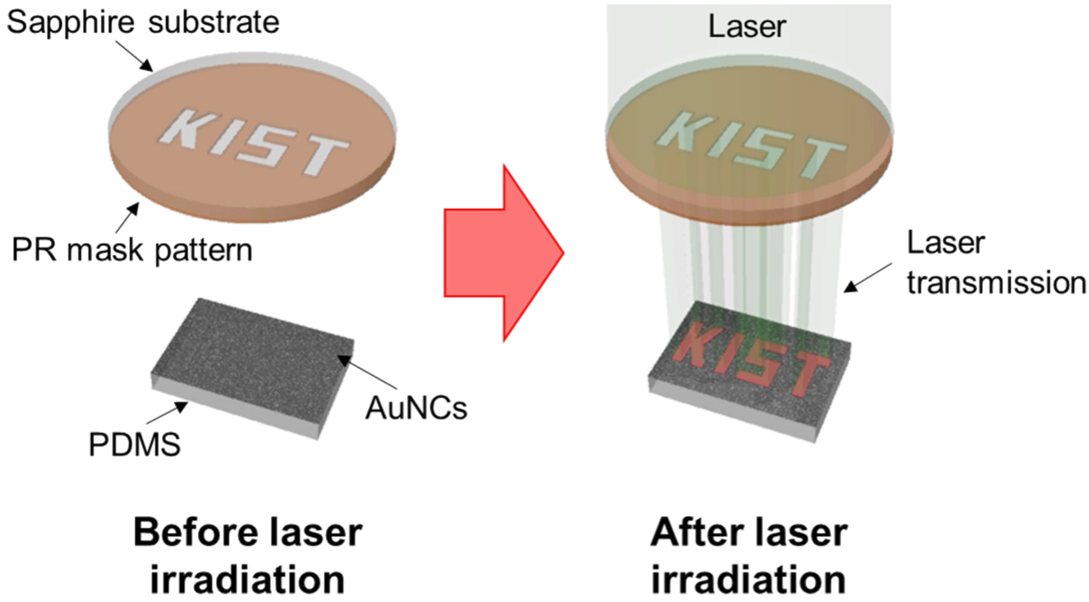

Fig. S13. Details of the "KIST" patterning processes.

In order to pattern the AuNS, we have used a photoresist patterned mask (letter "KIST") that facilitated the photolithography process. We placed the PR patterned mask on the AuNCs/PDMS and the PR patterned mask is attached. After that, the excimer laser is irradiated on the sapphire substrate. In a twinkling, AuNCs absorbs the laser transmitted through sapphire and the PR patterned mask. Finally, their morphology changes to AuNSs (letters "KIST").

14. Extinction properties of AuNS as a function of stress

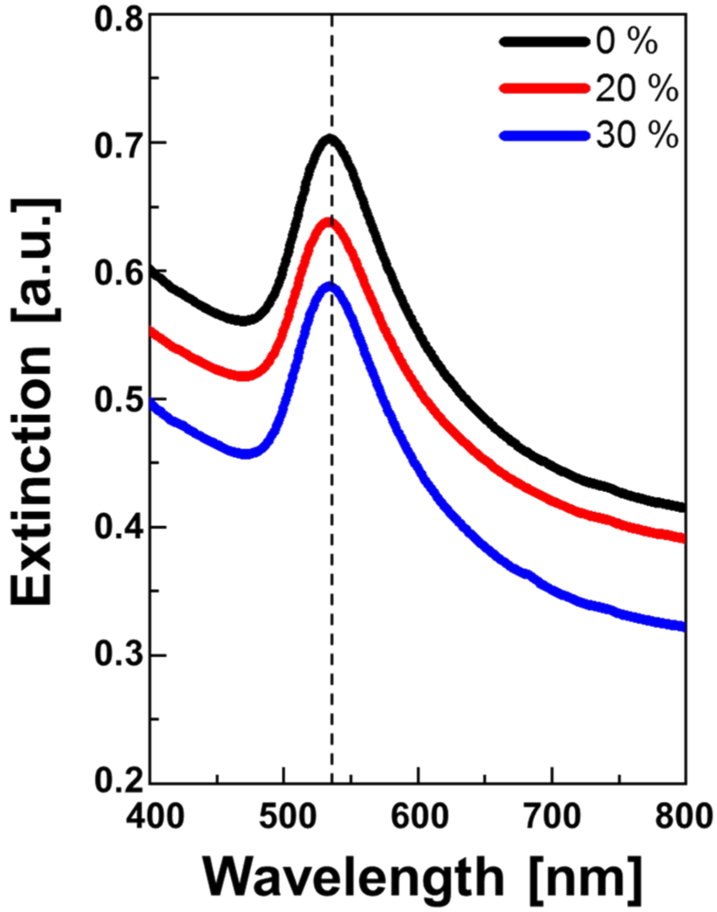

Fig. S14. Extinction properties of AuNS as a function of stress (0%: initial state, 20%: displacement 6 mm, 30%: displacement 9 mm)

15. COMSOL modeling condition of the AuNC on the sapphire structure.

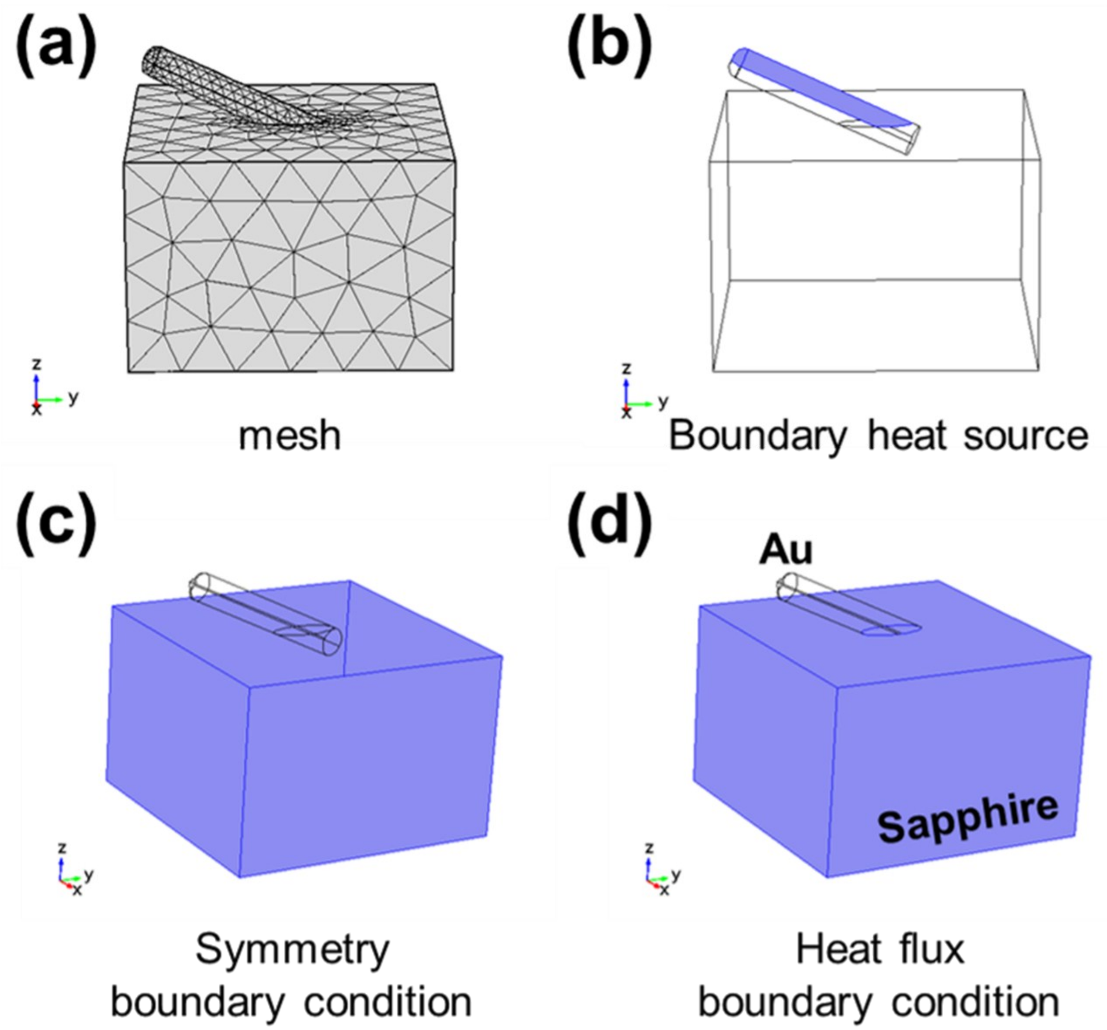

Fig. S15. Modeling conditions of the Au NC/sapphire structure (Au thickness 170 nm, Au diameter 30 nm, and sapphire thickness 200 nm). a) mesh b) boundary heat source, c) symmetry boundary condition, d) heat flux boundary condition.

16. Parameters of the excimer laser for COMSOL simulation.

Name	Expression	Description
ED	75 [mJ·cm^{-2}]	Energy density
Tau	24 [ns]	Laser pulse time
T_0	293 [K]	Ambient temperature
PD	$\frac{ED}{tau}(t \leq 24\,ns)$ [W·m^{-2}]	Input power

Tab. S1. Parameters of the excimer laser for COMSOL simulation.

17. Materials properties for COMSOL simulation.

Name	**Heat capacity [J·(kg·K)$^{-1}$]**	**Density [kg·m^{-3}]**	**Thermal conductivity [W·(m·K)$^{-1}$]**
Au	129	19300	317
Sapphire	1000	3980	25.12 (T < 673 K) 12.56 (T > 673 K)

Tab. S2. Materials properties for COMSOL simulation.